

Spatial control of a classical electron state in a Rydberg atom by adiabatic synchronization

E. Grosfeld and L. Friedland

Racah Institute of Physics, Hebrew University of Jerusalem, Jerusalem 91904, Israel

(Received 12 November 2001; published 10 April 2002)

An adiabatic synchronization approach is used to control orbital eccentricity and inclination of a highly excited electron in a hydrogen atom. The approach is based on persisting nonlinear phase locking (autoresonance) between spatially uniform, chirped frequency oscillating electric field, and the classical Keplerian motion of the electron in the atom. Efficient control in three dimensions is achieved by slow passage through and capture into different resonances. Scenarios guaranteeing the capture and continuing synchronization in the system are outlined, all requiring the driving field amplitude to exceed a threshold. The threshold scales as $A^{3/4}$, where A is the sweep rate of the driving frequency at resonance. The adiabatic synchronization allows one to accelerate the electron gradually by using dipolar fields, until approaching the stochastic ionization limit.

DOI: 10.1103/PhysRevE.65.046230

PACS number(s): 05.45.Xt, 32.80.Rm

I. INTRODUCTION

Extensive theoretical and experimental work in the last three decades has been devoted to the study of dynamics of highly excited (Rydberg) atoms in microwave fields. This research was stimulated by experiments of Bayfield and Koch [1], measuring the probability of ionization of beams of highly excited hydrogen atoms passing through a microwave cavity. Leopold and Percival [2] applied a classical approach to microwave ionization of Rydberg hydrogen atoms and described the electron as moving on a classical orbit in an oscillating, linearly polarized electric field. Results of Monte-Carlo simulations of ionization based on this model were close to the experimental results of Bayfield and Koch. Meerson, Oks, and Sasorov [3] suggested a mechanism for the ionization of Rydberg atoms based on stochastic instability of the classical motion of the electron in the atom. Since these early works, the use of classical (and semiclassical) ideas in studying highly excited perturbed atomic and molecular systems gained momentum covering various issues of microwave ionization (for a review see Ref. [4]), as well as many other aspects, such as nonspreading wave packets associated with resonantly driven Rydberg states [5,6], chaotic dynamics with broken time-reversal symmetry [7], effects of elliptical polarization of the microwave fields [8], and use of Rydberg atoms as sensitive magnetic probes [9], to name just few recent examples.

One of the classical ideas applied to Rydberg atoms was the use of the synchronization (phase locking) phenomenon to *control* the electron state of the atom by chirped frequency radiation. The idea was based on creating an atomic state, such that the Keplerian motion of the electron in the atom was phase locked with an external oscillating electric field having chirped frequency. When such a phase locking was sustained continuously, despite the variation of the driving frequency, one could observe adiabatic adjustment of the electron state (its energy, for example) to stay in resonance with the driving perturbation. The first application of this approach to Rydberg atoms [10] used a simplified one-dimensional (1D) electron orbit model and showed that the mechanism of phase locking in the system was similar to that used in a certain type of charged particle accelerator [11], so

the term *Rydberg accelerator* was suggested for this application. Later, a similar idea was suggested for exciting and controlling vibrational states of diatomic molecules [12]. In addition to limitations imposed by 1D modeling, exact initial matching between the characteristic frequency of the atomic or molecular system and that of the driving field was assumed in these studies. This approach required fine initial tuning of the driving frequency, while the continuing phase locking in the system was observed only for some range of initial phases of the driving field.

In the present work we propose the use of *passage through* resonance, as a tool to phase lock efficiently with the driving perturbation, *regardless* of the initial driving phase. We shall also generalize to 3D and show how the synchronization via passage through resonance allows to fully control the dynamics of the driven system (orbital eccentricity and inclination) by slowly varying parameters of the driving field. These ideas have been already used successfully in both theory and experiments in other applications. Recent examples are excitation and control of nonlinear waves [13], creation of nontrivial 2D vortex states in fluids [14,15], and pure electron plasmas, and the explanation of observed large eccentricities of transneptunian objects (Plutinos) in the solar system [16,17]. The elements of the analysis in the latter work are applied here to a related problem of adiabatically driven Rydberg atom in its full 3D complexity. The scope of our presentation will be as follows. We shall consider spatially uniform, quasimonochromatic oscillating electric fields with slowly varying frequencies, passing through different $l:m$ resonances in the system (i.e., $l\Omega_K = m\omega$, Ω_K and ω being the Keplerian frequency of the electron and the frequency of the driving field). In particular, Secs. II and III identify 2:1 and 1:1 resonances with linearly polarized driving electric fields as convenient candidates for adiabatic control of the dynamics of Rydberg atoms. We shall show that in both cases the theory reduces to studying the same pair of explicitly time dependent phase-amplitude evolution equations with a *single* parameter (rescaled driving amplitude). We shall also show that this system yields efficient resonant trapping, followed by continuing phase locking (synchronization) with the driving field, provided this parameter exceeds a threshold. In Sec. IV, we discuss the validity criteria

of our analysis and, finally, Sec. V presents our conclusions.

II. 2:1 RESONANCE, ECCENTRICITY CONTROL, AND THRESHOLD PHENOMENON

Our starting point is the classical Hamiltonian of an electron in a hydrogen atom perturbed by a linearly polarized quasimonochromatic oscillating electric field (along the Z direction)

$$H = H_0 + Z\mu \cos \Psi, \quad (1)$$

where $H_0 = p^2/2 - 1/r$ is the unperturbed Hamiltonian, μ represents the amplitude of the driving field, Ψ is its phase, and $\omega(t) = d\Psi/dt$ is the time dependent frequency of the perturbation. We shall consider the case when the unperturbed electron starts on a circular orbit of radius r_0 and angular frequency $\Omega_0 = e(m_e r_0^3)^{-1/2}$. Note that, for convenience, we replaced e , $m_e = 1$ in the Hamiltonian, equivalent to using dimensionless time $t \rightarrow \Omega_0 t$, dimensionless coordinates $(X, Y, Z) \rightarrow (X, Y, Z)/r_0$ and radius $r \rightarrow r/r_0$, and normalizing the momentum $\vec{p} \rightarrow \vec{p}/(m_e \Omega_0 r_0)$. We also introduced dimensionless field amplitude $\mu \rightarrow (r_0^2/e)E_0$ in the Hamiltonian, with E_0 being the original amplitude. All frequencies in the problem are dimensionless and correspond to original frequencies normalized with respect to Ω_0 . For simplicity, we use linear frequency chirp, $\omega(t) = \omega_0 - At$, where A is the chirp rate and ω_0 corresponds to normalized angular frequency (or its harmonics) of the unperturbed electron, so, for example, $\omega_0 = 2$ if the 2:1 resonance is considered. Note that in dimensionless notations, A corresponds to original A/Ω_0^2 . We shall also assume adiabaticity, i.e., $\kappa = |A|^{1/2}/\omega_0 \ll 1$, as well as that $\mu \ll 1$, so the driving field can be treated as a perturbation. But, we shall use $\kappa/\mu \ll 1$, and, therefore, μ will always be the largest of the two small parameters in the problem.

It is convenient, at this stage, to transform to the action-angle variables $I_{1,2,3}$ and $\theta_{1,2,3}$ [18] of the unperturbed problem. The *normalized* actions are related to different physical quantities, $I_1 = M_z/M_0$, $I_2 = M/M_0$, and $I_3 = M_0^{-1}(m_e e^4/2|E|)^{1/2}$, where M is the magnitude of the total angular momentum, M_z is the momentum projection on the Z axis (the direction of polarization of the driving electric field), E is the energy of the unperturbed electron, and the normalization constant $M_0 = m_e \Omega_0 r_0^2$ is the initial angular momentum. The angles $\theta_{1,2}$ are Euler's angles (see Fig. 1) $\theta_1 = \phi$, $\theta_2 = \psi$. The third Euler's angle i (inclination), eccentricity ε , and normalized semimajor axis a of the ellipse are simply related to the dimensionless actions, i.e., $\cos i = I_1/I_2$, $\varepsilon^2 = 1 - I_2^2/I_3^2$, and $a = I_3^2$.

Next, we transform the Hamiltonian (1) to the action-angle variables [3]

$$H = H_0 + \mu H_1 \cos \Psi, \quad (2)$$

where the unperturbed part $H_0 = -1/2I_3^2$ (see, e.g., Ref. [18]), $H_1 = \sin i \sum_{k=1}^{\infty} (a_k \cos k\theta_3 \sin \theta_2 + b_k \sin k\theta_3 \cos \theta_2)$, and coefficients a_k and b_k are $a_k = (2a/k)J'_k(k\varepsilon)$; $b_k = [2a(1$

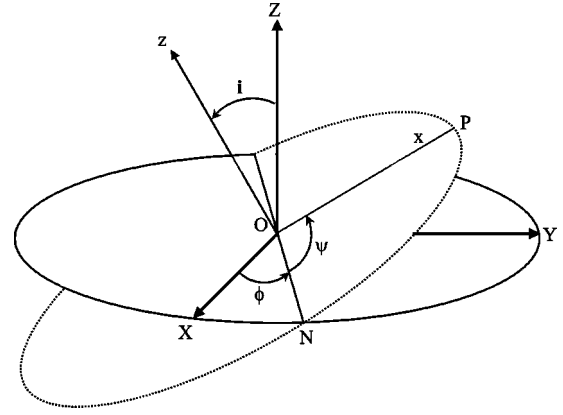


FIG. 1. The Keplerian ellipse (dotted line) and Euler's angles ϕ , ψ , and i . The electric field polarization is in the Z direction in the rest frame (X, Y, Z) . Points P and N denote periastron and ascending node in astronomical notations. Axes x, y (not shown), and z are attached to the ellipse.

$-\varepsilon^2)^{1/2}] / k\varepsilon J'_k(k\varepsilon)$ [19]. Here $J_k(x)$ and $J'_k(x)$ are the Bessel function of integer order k , and its derivative.

At this point, we proceed to studying passage through resonance in our driven system. Recall that the atomic electron is on a circular orbit initially (i.e., $\varepsilon = 0$ at some large negative t) and its Keplerian frequency is out of resonance (see below) with the driving perturbation. Since the driving field is small, we focus on the case of small eccentricities ε initially. In this case $a_1 \approx b_1 \approx a$, $a_2 \approx b_2 \approx \varepsilon a/2$, while $O(a_{k>2}) \sim O(b_{k>2}) \sim O(\varepsilon^{k-1})$. We observe that only terms with a_2 and b_2 in the perturbed part of 2 are proportional to ε . We shall see below that this dependence on ε in the Hamiltonian yields efficient phase locking when the driving field oscillation passes the resonance associated with these terms. Consequently, in studying the phase locking in the system we retain the terms with $k=2$ only in H_1 . The resulting perturbed part of the Hamiltonian is

$$H' = \frac{\mu \sin i}{4} [(a_2 + b_2) \cos \Phi_+ + (a_2 - b_2) \cos \Phi_-], \quad (3)$$

where $\Phi_{\pm} = 2\theta_3 \pm \theta_2 - \Psi \mp \pi/2$. Furthermore, since $a_2 - b_2$ is small at small ε , we focus on the resonance associated with the term having coefficient $a_2 + b_2$ in H' above, i.e., arrive at the *single resonance* Hamiltonian

$$H_{sr} = H_0 + \frac{\mu \sin i}{4} (a_2 + b_2) \cos \Phi. \quad (4)$$

To lowest order in ε , H_{sr} has the form

$$H_{sr} = -\frac{1}{2I_3^2} + \frac{\mu \varepsilon a}{4} \sin i \cos \Phi, \quad (5)$$

where $\Phi = \Phi_+$. This Hamiltonian yields the following evolution equations:

$$\dot{I}_1 = 0, \quad (6)$$

$$\dot{I}_2 = \frac{\mu \varepsilon a}{4} \sin i \sin \Phi, \quad (7)$$

$$\dot{I}_3 = \frac{\mu \varepsilon a}{2} \sin i \sin \Phi; \quad (8)$$

$$\dot{\theta}_1 = -\frac{\mu \varepsilon a I_1}{4 I_2^2 \sin i} \cos \Phi,$$

$$\dot{\theta}_2 = \frac{\mu a}{4} \left(\frac{\varepsilon I_1^2}{I_2^3 \sin i} - \frac{I_2 \sin i}{\varepsilon I_3^2} \right) \cos \Phi,$$

$$\dot{\theta}_3 = \Omega_K + \frac{\mu}{4} \sin i \left(2 \varepsilon I_3 + \frac{I_2^2}{\varepsilon I_3} \right) \cos \Phi,$$

where $(\dots) = d(\dots)/dt$, and $\Omega_K = 1/I_3^3$ is the Keplerian frequency of the unperturbed electron.

Now, in agreement with the form of phase Φ , we seek passage through 2:1 resonance, i.e., $2\Omega_K = \omega_0$ at $t=0$ (recall that the driving frequency is $\Psi = \omega = \omega_0 - At$). Observe that Eqs. (6)–(8) yield two conservation laws

$$I_1 = I_{10}, \quad 2I_2 - I_3 = 1, \quad (9)$$

where initially (on the circular orbit), $I_{20} = I_{30} = 1$. Therefore, the problem reduces to a one-degree-of-freedom case characterized by, for example, I_3 and Φ . We write $I_3 = 1 + \delta I$, where δI is small in the initial evolution stage. Then $I_2 = 1 + \delta I/2$, $\varepsilon \approx \delta I^{1/2}$, $\sin i \approx (1 - I_{10}^2)^{1/2} = \sin i_0$, and, to lowest order in ε , our evolution equations yield

$$\delta \dot{I} = \frac{\mu \sin i_0}{2} \delta I^{1/2} \sin \Phi, \quad (10)$$

$$\dot{\Phi} = At - 6\delta I + \frac{\mu \sin i_0}{4} \delta I^{-1/2} \cos \Phi. \quad (11)$$

Finally, we use rescaled eccentricity $\Delta = \sqrt{6A}^{-1/4} \varepsilon$ as a new dependent variable instead of δI , introduce a new (slow) time variable $\tau = A^{1/2} t$, and obtain the following evolution equations:

$$\frac{d\Delta}{d\tau} = \eta \sin \Phi, \quad (12)$$

$$\frac{d\Phi}{d\tau} = \tau - \Delta^2 + \frac{\eta}{\Delta} \cos \Phi, \quad (13)$$

where $\eta = \sqrt{3/8A}^{-3/4} \mu \sin i_0$ is the rescaled driving amplitude.

The system (12), (13) comprises a pair of time dependent equations with a *single* parameter η . Note the presence of the characteristic term with Δ^{-1} in the phase equation in this system. This singular term is the direct consequence of leaving the $O(\varepsilon)$ term only in the single resonance Hamiltonian and plays a major role in the resonant phase locking phenomenon. Indeed, the form of the reduced evolution equa-

tions (12) and (13) is the same as that studied previously [20] and, thus we can use already known results. One of the important conclusions of that theory is that if one starts with small Δ at large negative τ , then, regardless of the initial value of Φ , the singular term with Δ^{-1} in the phase equation guarantees efficient trapping into resonance followed by continuing synchronization ($d\Phi/d\tau \approx 0$) in the system at $\tau > 0$ as well, provided the driving parameter is above a threshold. Numerically, the threshold is $\eta_{th} = 0.411$, while physical arguments yield a somewhat higher value $\eta_{th} = 3^{-3/4} = 0.439$. Therefore, by returning to our original parameters, we obtain the following scaling of the threshold driving amplitude with respect to the driving frequency chirp rate A , and initial inclination i_0 :

$$\mu_{th} = 0.67 (\sin i_0)^{-1} A^{3/4}. \quad (14)$$

The phase locking in our reduced system means that the phase mismatch Φ remains small at all times, i.e., at large positive τ , we obtain a monotonically increasing solution $\Delta^2 \approx \tau$, in other words, a monotonic increase of the eccentricity. Fully nonlinear treatment of the problem is necessary when the eccentricity becomes large. Such fully nonlinear theory of phase locked evolution can still be based on single resonance approximation. Its details are similar to those described in other applications (e.g., Ref. [10]) and we shall not present these details here. Nevertheless, we mention that the conservation laws (9) still hold within the single resonance approximation in the fully nonlinear regime, while phase locking $\dot{\Phi} \approx 2\dot{\theta}_3 + \dot{\theta}_2 - \omega(t) \approx 0$ is preserved, as long as additional conditions are satisfied (see the discussion of these conditions in Sec. IV). Then the approximate relation $2\Omega_K \approx \omega(t)$ is satisfied at later times, or

$$2/I_3^3 \approx 2 - At. \quad (15)$$

Thus, the synchronized state yields acceleration of the electron and gradual approach towards the ionization limit $I_3 \rightarrow \infty$ (see Sec. IV). The simple time dependence (15), in combination with the conservation laws (9), can be used for calculating the eccentricity of the phase locked state

$$\varepsilon^2 = 1 - I_2^2/I_3^2 = 1 - (1/4)(1/I_3 + 1)^2. \quad (16)$$

We obtain a growing solution for ε , asymptotically approaching $\varepsilon = (3/4)^{1/2}$ at $I_3 \rightarrow \infty$. Similarly, one can find the expression for the inclination of the orbit:

$$\cos i = I_1/I_2 = 2 \cos i_0 / (1 + I_3). \quad (17)$$

Therefore, the inclination angle increases as phase locking continues, approaching $\pi/2$ at $I_3 \rightarrow \infty$. Finally, the linear chirp of the driving frequency is not necessary for preservation of the phase locking in the system. Once trapped, one can use arbitrary, but sufficiently slow chirp form, i.e., replace At in Eq. (15) by any slow function $f(t)$ and even reverse the variation of the driving frequency [20]. In the latter case one will gradually return to a nearly original circular state as described by Eqs. (16) and (17).

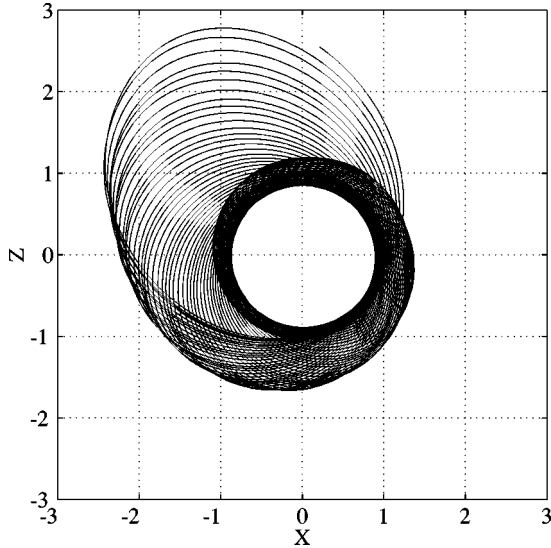


FIG. 2. The trajectory of the driven electron in the phase locked regime during passage through a 2:1 resonance with chirped frequency driving electric field. The chirp rate is $A=0.002$, driving parameter $\mu=0.015$, and inclination $i_0=\pi/2$ (driving field in the plane of the orbit). Initial orbit is circle $r=1$. One observes a gradual increase of eccentricity of the orbit synchronized with the driving field, as well as slow precession around the origin.

Now, we discuss evolution of canonical angles in the phase locked state when the average value of Φ remains small. The phase locking yields one connection between θ_1 and θ_2 . On the other hand, when Φ is small, one can replace $\cos \Phi$ in the first equation in Eq. (8) by unity, yielding $\dot{\theta}_1 = -\mu \epsilon a I_1 / 4 I_2^2 \sin i$, which describes a slow and slowly varying precession of the orbital plane around the direction of the driving electric field. This motion completely defines both canonical angles θ_1 and θ_2 . The evolution of the third angle is approximately given by the slowly varying Keplerian frequency of the electron, i.e., $\dot{\theta}_3 \approx 1/I_3^3$ [see the third equation in Eq. (8)]. Thus, the evolution of all degrees of freedom is determined. Remarkably, in the synchronized regime, the complete motion can be approximately derived from simple algebraic relations (15)–(17).

At this stage, we illustrate our theory by numerical examples. Figure 2 shows the trajectory of the electron in the phase locked regime as obtained by passage through 2:1 resonance. We show the case of chirp rate $A=0.002$, driving parameter $\mu=0.015$, and $i_0=\pi/2$ (driving field in the plane of the orbit). The threshold driving parameter in this case was $\mu_{th}=0.0063$. We used a full Hamiltonian (1) in calculating this trajectory. One can see a slow increase of eccentricity as well as precession of the trajectory described above. Further results of these calculations are given in Fig. 3 showing the evolution of eccentricity of the orbit. The solid line in the figure represents the numerical solution of the exact problem described by Eq. (1), the dotted line is obtained by solving reduced weakly nonlinear systems (12) and (13), while the dashed line is given by the algebraic equation (16). We see a gradual increase of the eccentricity beyond the linear resonance, indicating continuing phase locking in the

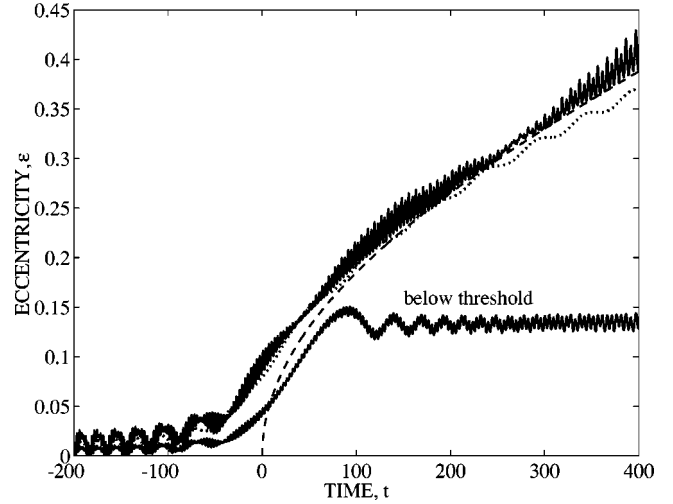


FIG. 3. The evolution of eccentricity of the orbit. The parameters are as in Fig. 2. The solid line: numerical solution of the problem described by the exact Hamiltonian. The dotted line is given by a reduced weakly nonlinear system. The dashed line represents algebraic approximation. The lowest curve represents a solution of the exact problem with the same parameters, but $\mu=0.006$, i.e., below the synchronization threshold ($\mu_{th}=0.0063$).

system, and generally good agreement between different approximations. In addition, the lowest curve in the figure represents the solution of the exact problem for the same initial conditions and parameters as previously, but with $\mu=0.006$, i.e., below the threshold. The eccentricity saturates at some value in this case, as the phase locking is destroyed beyond the linear resonance. Next, Fig. 4 compares scalings of the threshold for synchronization as obtained in calculations using the exact Hamiltonian [$(\Delta) i_0=\pi/2$, $(\circ) i_0=\pi/4$, $(\square) i_0=\pi/6$] and those given by Eq. (14) (straight lines). Again, one can see a good agreement between the two results. This

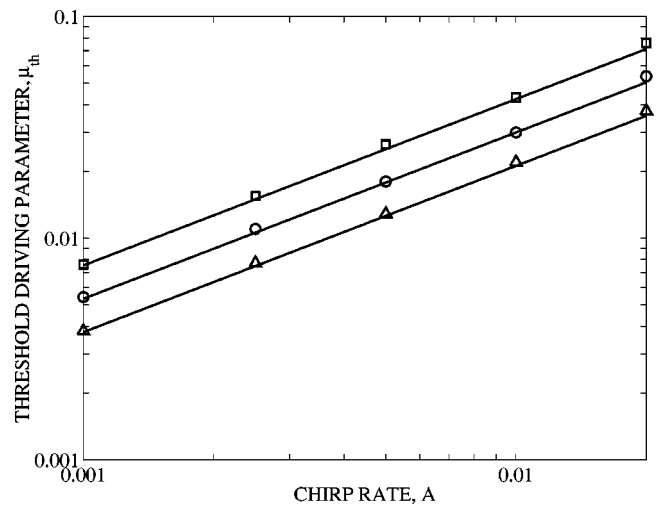


FIG. 4. The threshold driving parameter for synchronization μ_{th} (circles) vs driving frequency chirp rate A for three different initial inclinations [$(\Delta) i_0=\pi/2$, $(\circ) i_0=\pi/4$, $(\square) i_0=\pi/6$], as obtained in calculations using the exact Hamiltonian. The solid lines represent results given by Eq. (14).

completes our first application of the adiabatic control of the electron state in the Rydberg atom by synchronization.

III. 1:1 RESONANCE AND INCLINATION CONTROL

We have seen in Sec. II how passage through 2:1 resonance, results in efficient trapping into resonance followed by continuing synchronization with the drive, provided one uses *small eccentricity* initial condition ($\varepsilon_0 \approx 0$) and if the driving amplitude is above a threshold. We have left the $k=2$ term only in H_1 in Eq. (2), i.e., constructed a single resonance Hamiltonian for studying this phenomenon. This choice of resonance is not the only one yielding efficient trapping. We shall show here that passage through 1:1 resonance can be also used for achieving a similar goal, if, initially, one has *small inclination* ($i_0 \approx 0$) of the orbit, i.e., the driving field is nearly normal to the orbital plane. We shall see that the corresponding single resonance Hamiltonian will also lead to a proper *singular term* in the phase mismatch evolution equation for efficient capture into resonance. Let us consider this problem in more detail. Now, we leave the $k=1$ term only in Eq. (2). The resulting perturbed part of the Hamiltonian is

$$H' = \frac{\mu \sin i}{4} [(a_1 + b_1) \cos \Phi_+ + (a_1 - b_1) \cos \Phi_-], \quad (18)$$

where $\Phi_{\pm} = \theta_3 \pm \theta_2 - \Psi \mp \pi/2$. We focus again on the resonance associated with the first term in Eq. (18), i.e., arrive at the single resonance Hamiltonian

$$H_{sr} = H_0 + \frac{\mu \sin i}{4} (a_1 + b_1) \cos \Phi, \quad (19)$$

where the phase mismatch is $\Phi \equiv \Phi_+$. Finally, for simplicity, consider the case of initially nearly circular orbit, i.e., $\varepsilon_0 \approx 0$. Then, in the initial excitation stage, H_{sr} can be written as

$$H_{sr} \approx -\frac{1}{2I_3^2} + \frac{\mu a}{2} i \cos \Phi, \quad (20)$$

where we approximated $\sin i = \sqrt{1 - I_1^2/I_2^2}$ by i .

The Hamiltonian (20) yields the following evolution equations for our action-angle variables:

$$\begin{aligned} \dot{I}_1 &= 0, \\ \dot{I}_2 &= \frac{\mu a i}{2} \sin \Phi, \\ \dot{I}_3 &= \frac{\mu a i}{2} \sin \Phi; \\ \dot{\theta}_1 &= -\frac{\mu a I_1}{2I_2^2} \cos \Phi, \end{aligned} \quad (21)$$

$$\dot{\theta}_2 = \frac{\mu a}{2} \frac{I_1^2}{I_2^3 i} \cos \Phi, \quad (22)$$

$$\dot{\theta}_3 = \Omega_K + \mu I_3 i \cos \Phi.$$

We see that I_1 and $I_2 - I_3$ are conserved. Therefore the problem again reduces to a one-degree-of-freedom system for a canonical pair, say I_2 and Φ . Furthermore, initially, $I_{10} \approx I_{20} = I_{30}$ ($i_0 \approx 0, \varepsilon_0 = 0$) and, therefore, at later times,

$$I_1 = I_{10} \approx 1, \quad I_2 \approx I_3. \quad (23)$$

In other words, the orbit remains nearly circular and only its inclination changes in time. If we write $I_2 = I_{10} + \delta I$, then, for small i , one has $i^2 = 1 - I_1^2/I_2^2 \approx 2\delta I$. Then, to lowest order in δI , the canonical system for I_2 and Φ is

$$\dot{I}_2 = \delta \dot{I} = \frac{\mu}{2} i \sin \Phi, \quad (24)$$

$$\dot{\Phi} \approx \Omega_K - \omega(t) + \frac{\mu}{2i} \cos \Phi. \quad (25)$$

If one further expands $\Omega_K = I_3^{-3} = I_2^{-3} \approx I_{10}^{-3} - 3\delta I$, uses $\omega(t) = \omega_0 - At$, where $\omega_0 = \Omega_{K0} = I_{10}^{-3}$, and uses i as an independent variable instead of δI , one has

$$\dot{i} = \frac{\mu}{2} \sin \Phi, \quad (26)$$

$$\dot{\Phi} \approx At - \frac{3}{2} i^2 + \frac{\mu}{2i} \cos \Phi. \quad (27)$$

Now, we introduce the slow time $\tau = A^{1/2}t$, rescaled inclination $\Delta = (3/2)^{1/2}i/A^{1/4}$ and arrive at the same reduced single parameter systems (12) and (13), where the rescaled driving parameter is $\eta = \sqrt{3/8}A^{-3/4}\mu$. Interestingly, this is the same value as for the 2:1 resonance problem described above, for initial inclination of $\pi/2$. The corresponding threshold for trapping into 1:1 and synchronization is [compare to Eq. (14)]

$$\mu_{th} = 0.67A^{3/4}. \quad (28)$$

At this point we have found conditions for capture into resonance and synchronization. The aforementioned threshold phenomenon was described in terms of weakly nonlinear theory. When our system is captured into resonance, the inclination grows with the decrease of the driving frequency and, at some point, one must switch to a fully nonlinear theory of the phase locked state. This theory is similar to that given elsewhere [10] and we shall not present its details here. Nonetheless, one can show that once started, the phase locking $\dot{\Phi} = \dot{\theta}_3 + \dot{\theta}_2 - \omega(t) \approx 0$ continues, under additional conditions, in the fully nonlinear stage as well. Then $I_3^{-3} \approx I_{30}^{-3} - At \approx 1 - At$, so

$$\cos i = I_1/I_2 \approx 1/I_3 \approx (1 - At)^{1/3}. \quad (29)$$

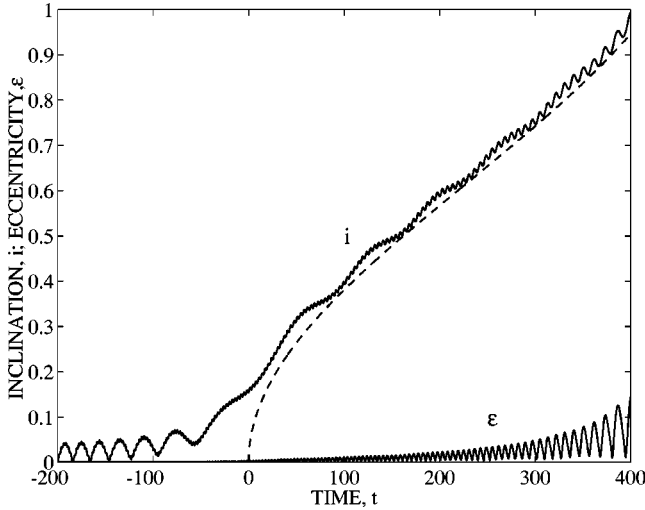


FIG. 5. The evolution of inclination i and eccentricity ϵ in the process of passage through a 1:1 resonance with the driving field having polarization perpendicular to the initial plane of the orbit. Exact Hamiltonian (1) was used in the calculations, chirp rate was $A=0.002$, and driving parameter $\mu=0.015$. The dashed line: algebraic approximation Eq. (29) beyond the linear resonance.

We see that the inclination i grows in time and approaches $\pi/2$, i.e., the orbital plane rotates to align with the direction of the driving field. The orbit, at the same time, maintains its nearly circular form, as the phase locked electron is accelerated and approaches the ionization limit. We illustrate all these conclusions in Fig. 5, showing the evolution of inclination and eccentricity in the process of passage through 1:1 resonance. The results were obtained by using equations given by exact Hamiltonian (1), chirp rate $A=0.002$, and driving parameter $\mu=0.015$ (the threshold value in this case is $\mu_{th}=0.0063$). We see that, as predicted, the eccentricity remains small, while the inclination angle grows in the phase locked state, nearly reaching $\pi/3$ at $t=400$ in this example, and closely following the result predicted by Eq. (29) (the dashed line) beyond the linear resonance.

IV. DISCUSSION

Now, we discuss the validity of approximations of our theory. The isolated resonance approximation used above is valid as long as $\nu \ll \omega(t)$, where ν is the characteristic frequency of small phase oscillations in the nonlinearly phase locked regime [3]. If, in the process of adiabatic control, one approaches the stage where this condition is violated, the synchronized slow evolution described above is replaced by stochastic instability and ionization of the atom for some trajectories, due to resonance crossings. The frequency ν of the trapped phase oscillations can be found by using appropriate single resonance Hamiltonians [i.e., Eqs. (4) and (19)]. Indeed, we write the following evolution equation equations associated with these Hamiltonians

$$\frac{dI_3}{d\tau} = \frac{\mu l \sin i}{4} R_l \sin \Phi, \quad \frac{d\Phi}{d\tau} \approx \frac{l}{I_3^3} - \omega(t), \quad (30)$$

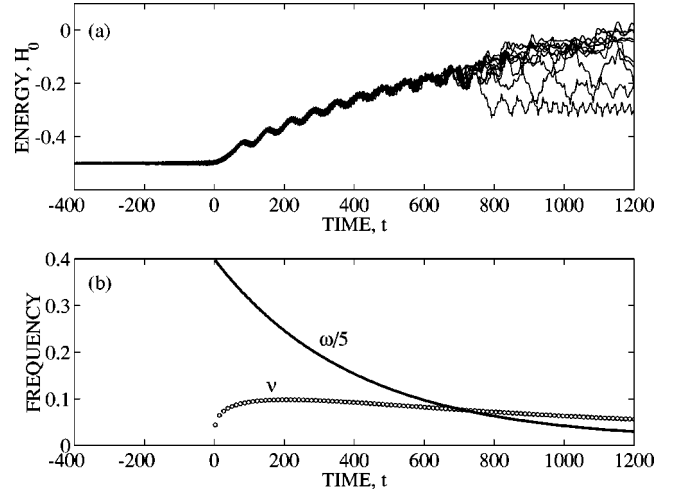


FIG. 6. Transition to stochastic instability by passage through a 2:1 resonance. (a) The unperturbed part H_0 of the exact Hamiltonian versus time for 10 numerical runs with the same initial conditions ($r=1, i_0=\pi/2$) as in Fig. 2, but different, equally spaced on $[0, 2\pi]$ initial differences between the phase of the Keplerian motion and that of the driving field. One observes that all trajectories are similar in the synchronized stage despite initial phase differences, until the stochasticity threshold is reached at $t \approx 700$. (b) The frequency ν (\circ) of small phase oscillations of the phase locked state and the driving frequency ω (solid line) versus time. The transition to instability and dephasing take place when $\nu \approx \omega(t)/5$.

where $l=1,2$ corresponds to 1:1 and 2:1 resonance cases described above, while $R_l=(a_l+b_l)$. Also, assuming a strongly nonlinear stage, we have neglected small interaction terms in the second equation in Eq. (30). Differentiation of the second equation in Eq. (30) and use of the first equation then yields

$$\frac{d^2\Phi}{d\tau^2} \approx A - \nu^2 \sin \Phi, \quad (31)$$

where $\nu^2 = 3l^2 \mu \sin i / 4I_3^4 (a_l + b_l)$. This equation describes a nonlinear pendulum (ν is the slowly varying characteristic frequency of small oscillations of the pendulum) under the action of a small constant torque. Thus, the condition for the onset of stochastic instability (leading to ionization for some trajectories) becomes

$$\frac{3l^2 \mu \sin i}{4I_3^4} (a_l + b_l) = \gamma \omega^2(t), \quad (32)$$

where γ is some number between, say 0.1 and 1.0. Assuming that one approaches this stochastic transition limit adiabatically through the synchronized state, we can estimate the time dependent parameters in this formula by using Eqs. (16), (17), or (29). We have tested condition (32) numerically and show one of these tests in Figs. 6(a) and 6(b). Figure 6(a) shows transition to stochastic instability in the case of synchronization by passage through 2:1 resonance with an oscillating electric field polarized linearly in the orbital plane. The figure shows the unperturbed part H_0 of the exact

Hamiltonian (1) versus time for 10 numerical runs with the same initial conditions ($r=1, i_0=\pi/2$) as in Fig. 2, but different, equally spaced on $[0, \pi]$ initial differences between the phase of the Keplerian motion and that of the driving field. We used the driving frequency $\omega(t)=D+(2-D)\exp(-At/2)$ with $D=0.05$, $A=0.005$, and driving amplitude parameter $\mu=0.013$ in these calculations, so the resonance passage occurred at $t=0$. One observes that despite the initial phase difference, all trajectories are synchronized after passage through resonance until the stochasticity threshold is reached at $t\approx 700$. The phase locking discontinues beyond this time and, later, some trajectories reach ionization limit. Figure 6(b) compares the frequency ν (\circ) of small phase oscillations in the phase locked state with the driving frequency (solid line) as functions of time. One can see in the figures that the transition to stochastic instability takes place when $\nu\approx\omega(t)/5$. We also found that $\nu\approx\omega(t)/5$ was a good criterion for transition to stochasticity for a broad range of values of the driving parameter and chirp rate.

In addition to the single resonance condition $\nu\ll\omega(t)$, the driving frequency must satisfy the adiabaticity condition

$$|\dot{\omega}|/\nu^2=A/\nu^2\ll 1. \quad (33)$$

Previously, we have mentioned condition $\kappa^2=A/\omega_0^2\ll 1$, but, since $\nu\ll\omega(t)$, Eq. (33) is a stronger inequality. The reason for demanding Eq. (33) at this stage is seen from Eq. (31). Indeed, this equation describes a quasiparticle moving in an effective tilted cosine potential

$$V_{\text{eff}}=-A\Phi-\nu^2\cos\Phi. \quad (34)$$

This potential possesses minima only if the tilting coefficient A is not too large, i.e., when $\nu^2>A$. The existence of the potential minima is necessary for having trapped oscillations of Φ , corresponding to phase locked oscillations in our dynamical problem. Thus, Eq. (33) at all times is necessary for having persisting phase locking in our driven atomic system.

Finally, the quantum mechanics imposes the constraint on the principle quantum number $n=M_0I_3/\hbar\ll 1$ (recall that we use dimensionless actions $I_{1,2,3}$ normalized with respect to the angular momentum M_0 of the initial orbit), and possibly other constraints, which are still unknown.

V. CONCLUSIONS

(i) We have studied passage through resonances and synchronization of the electron state of a Rydberg atom driven by linearly polarized oscillating electric field with slowly decreasing frequency. Two possibilities exist leading to efficient (100%) capture into resonance regardless the value of the initial driving phase. In both cases the electron is accel-

erated gradually approaching the ionization limit with the decrease of the driving frequency.

(ii) The first scenario requires starting on a circular orbit and passage through 2:1 resonance with the driving field having a finite projection in the plane of the initial orbit. The capture into resonance in this case is followed by continuous phase locking in the system despite slow variation of the driving frequency provided the driving amplitude is above a threshold. The threshold amplitude scales as $A^{3/4}$, A being the chirp rate of the driving frequency. The continuing phase locking in the system means slow evolution of the electron orbit (the eccentricity and inclination) in three dimensions, reflecting self-adjustment of the electron state for staying in resonance with the driving field.

(iii) The second scenario involves passage through 1:1 resonance when the driving field polarization is nearly perpendicular to the plane of initially circular orbit. This route also leads to efficient capture into resonance, followed by continuing synchronization, provided the driving field amplitude is above the threshold, which again scales as $A^{3/4}$. When trapped into resonance, the orbit, in this case, remains nearly circular at all times, while inclination of the orbit varies slowly in time with the decrease of the driving frequency.

(iv) The two scenarios above can be used separately, in succession, or simultaneously for efficient three-dimensional control of the electron state of the Rydberg atom. This control process is reversible, i.e., the electron orbit can be returned back to a nearly initial state by simply reversing the direction of variation of the driving frequency $\omega(t)$.

(v) Two conditions must be satisfied for the validity of our approach to manipulation of Rydberg atoms. One condition is the continuing satisfaction of the single resonance approximation, i.e., $\nu\ll\omega(t)$, where ν is the frequency of small phase oscillations in the phase locked state. If, in the phase locked regime with the decrease of the driving frequency, one violates this condition, the phase locking in the system is destroyed and stochastic instability, leading to ionization for some trajectories, takes place. The second condition is the adiabaticity (33), guaranteeing continuing phase locking in the system.

(vi) Finally, quantum mechanics requires the principal quantum number n to be much greater than unity to justify our classical description of the dynamics. Additional quantum-mechanical conditions may exist, but presently are unknown, since there exists no theory studying the transition from classical to quantum regime in the driven phase locked states described here. Development of such a theory seems to be an interesting goal for future work.

ACKNOWLEDGMENT

We acknowledge the support of the US-Israel Binational Science Foundation (Grant No. 1998474).

[1] J.E. Bayfield and P.M. Koch, Phys. Rev. Lett. **33**, 258 (1974).
 [2] J.G. Leopold and I.C. Percival, Phys. Rev. Lett. **41**, 944 (1978).

[3] B.I. Meerson, E.A. Oks, and P.V. Sasorov, Pis'ma Zh. Eksp. Teor. Fiz. **29**, 79 (1979) [JETP Lett. **29**, 72 (1979)].

[4] P.M. Koch and K.A.N. van Leeuwen, Phys. Rep. **255**, 289

- (1995).
- [5] I. Bialynicki-Birula, M. Kalinski, and J.H. Eberly, *Phys. Rev. Lett.* **73**, 1777 (1994).
- [6] A. Buchleitner, K. Sacha, D. Delande, and J. Zakrzewski, *Eur. Phys. J. D* **5**, 145 (1999).
- [7] K. Sacha, J. Zakrzewski, and D. Delande, *Phys. Rev. Lett.* **83**, 2922 (1999).
- [8] E. Oks, J.E. Davis, and T. Uzer, *J. Phys. B* **33**, 207 (2000).
- [9] E. Oks and T. Uzer, *J. Phys. B* **33**, 2207 (2000).
- [10] B. Meerson and L. Friedland, *Phys. Rev. A* **41**, 5233 (1990).
- [11] K.S. Golovanivskii, *Fiz. Plasmy* **11**, 295 (1985) [*Sov. J. Plasma Phys.* **11**, 171 (1985)].
- [12] W.K. Liu, B. Wu, and J.M. Yuan, *Phys. Rev. Lett.* **75**, 1292 (1995).
- [13] L. Friedland and A.G. Shagalov, *Phys. Rev. Lett.* **81**, 4357 (1999).
- [14] J. Fajans, E. Gilson, and L. Friedland, *Phys. Rev. Lett.* **82**, 4444 (1999).
- [15] L. Friedland and A.G. Shagalov, *Phys. Rev. Lett.* **85**, 2941 (2001).
- [16] R. Malhotra, *Nature (London)* **365**, 819 (1993).
- [17] L. Friedland, *Astrophys. J. Lett.* **547**, L75 (2001).
- [18] H. Goldstein, *Classical Mechanics* (Addison-Wesley, Reading, MA, 1980).
- [19] L.D. Landau and E.M. Lifshitz, *The Classical Theory of Fields* (Pergamon, Oxford, 1975), pp. 181–182.
- [20] L. Friedland, *Phys. Rev. E* **59**, 4106 (1999).